THE ASTROPHYSICAL JOURNAL, 409:422–428, 1993 May 20

DETECTION OF CIRCUMSTELLAR GAS ASSOCIATED WITH GG TAURI[1]

M. F. SKRUTSKIE,[2] R. L. SNELL,[2,3] K. M. STROM,[2] S. E. STROM,[2] AND S. EDWARDS[4]
Five College Astronomy Department, University of Massachusetts, Amherst, MA 01003
Y. FUKUI AND A. MIZUNO
Department of Astrophysics, Nagoya University, Chikusa-ku, Nagoya 464-01, Japan
M. HAYASHI
Department of Astronomy, University of Tokyo, Yayoi, Bunkyo, Tokyo 113, Japan
AND
N. OHASHI
Nobeyama Radio Observatory, National Astronomical Observatory, Nobeyama, Minamisaku, Nagano 384-13, Japan
Received 1992 July 15; accepted 1992 November 4

ABSTRACT

We report detection of double-peaked ^{12}CO (1–0) emission ($\Delta v_{\rm FWHM} = 2.4$ km s^{-1}) centered on the young ($t \sim 3$ Myr) T Tauri star, GG Tau. The line profile can be modeled successfully by assuming that CO emission arises in an extended circumstellar disk, with half the emission arising inside a radius, r_0, where $400 < r_0 < 600$ AU (depending on the inclination of the GG Tau star/disk system to the line of sight). Our detection of ^{12}CO combined with our inability to measure C^{18}O bounds the observed gas mass between $2 \times 10^{-5} < M_{\rm gas}/M_\odot < 1.1 \times 10^{-3}$. However, an arbitrarily large amount of mass could reside within a small ($r \ll 200$ AU), optically thick region and would escape detection owing to beam dilution effects. Comparison of our estimated gas mass with the dust mass estimated from recent millimeter-continuum measurements over a region comparable to our 15″ beam yields a gas/dust ratio on the order of 10–100 times smaller than the interstellar value. Either (1) the gas/dust ratio is abnormally low, or (2) CO may no longer accurately trace the gas mass, either because it is dissociated, frozen onto grains, or because carbon is locked up in more complex molecules. Observations of CS (2–1) obtained simultaneously with our ^{12}CO measurements show no evidence of emission in excess of $T_A = 32$ mK (1 σ). Our derived upper limit to the CS emission implies a ratio N(CS)/N(CO) either comparable to its interstellar value in the event that ^{12}CO emission is optically thin, or smaller by a factor of ~ 10, if we adopt the upper limit to ^{12}CO optical depth derived from our C^{18}O upper limit.

Subject headings: circumstellar matter — radio lines: ISM — stars: individual (GG Tauri) — stars: pre–main-sequence

1. INTRODUCTION

Observations of young ($t < 3$ Myr), optically visible solar-type stars suggests that at least half are surrounded by massive disks (Strom et al. 1989). The most compelling evidence is provided by observation of large infrared excess emission above stellar photospheric values, which most plausibly arises from heated micron-sized circumstellar dust. To account for the observed infrared, submillimeter and millimeter-continuum excesses requires optical depths at wavelengths $\lambda > 100$ μm which imply visual extinctions $\tau_{\rm dust}(V) > 1000$ (Beckwith et al. 1990; Weintraub, Sandell, & Duncan 1989; Adams, Emerson, & Fuller 1990). The stars would be invisible if this dust were distributed spherically. However, dust confined to a disklike geometry can both provide the required infrared opacity and preserve an optically thin line of sight to the stellar photosphere (Kenyon & Hartmann 1987; Bertout, Basri, & Bouvier 1988; Adams, Lada, & Shu 1987). Moreover, the observed spectral energy distribution of the excess infrared emission ($\lambda \leq 100$ μm) closely approximates the spectral slope expected for geometrically thin, optically thick disks heated either radiatively, by the central solar-type star, or viscously, via accretion (e.g., Kenyon & Hartmann 1987; Lynden-Bell & Pringle 1974). Finally, the broad forbidden emission lines observed in large numbers of T Tauri stars lack redshifted emission components (e.g., Appenzeller, Jankovics, & Ostreicher 1984; Edwards et al. 1987). Because these features are believed to trace energetic winds extending to distances more than 10 AU from the stellar surface, the observed absence of redshifted emission suggests that we see only the approaching outflowing gas; the receding, redshifted component is hidden from view by an optically thick circumstellar disk of dimension $r \gg 10$ AU, whose opacity is almost certainly provided by micron-sized dust.

The above indirect, but compelling, evidence for circumstellar disks all derives from observation of emission from, or extinction by, small dust particles. However, in the interstellar medium, and at least initially in circumstellar disks, the mass in gas is expected to dominate that in dust by a factor of ~ 100 (e.g., Hildebrand 1983). At the high densities ($n \gg 10^6$ cm^{-3}) which obtain in circumstellar disks, the gas is almost certainly molecular except within several stellar radii of the star's surface. However, detection of molecular emission from circumstellar disks is extremely difficult, primarily because most young stars are still located within the confines of molecular clouds from which they form. Ambient molecular cloud emis-

[1] This contribution was carried out under the "common use" program of the 45 m radio telescope at Nobeyama.
[2] Physics and Astronomy Department, University of Massachusetts.
[3] Five College Radio Astronomy Observatory.
[4] Astronomy Department, Smith College.

sion dominates disk emission for measurements made with single-dish antennae, where the size of the beam (typically $\theta > 10''$) exceeds the expected disk size ($\theta < 5''$), even for objects located in the nearest star-forming complexes. Thus far, the only clear evidence of circumstellar gas confined to a disk surrounding a young, optically visible solar-type star comes from millimeter wave interferometer measurements of HL Tau. Observations of this star in ^{13}CO and $C^{18}O$ made at the Owens Valley Radio Observatory by Sargent & Beckwith (1991) effectively separate the small-scale, circumstellar emission peaked on the star from the relatively smooth emission from the ambient gas, and reveal a flattened, clumpy circumstellar structure in which the gas appears to be in Keplerian motion around the central star. The inferred gas mass is $\sim 0.1\ M_{\odot}$.

Further observations of the gas component of circumstellar disks are essential. First, observation of spectral lines arising in the gas can provide a *kinematic signature* of a disk, the most compelling evidence of such structures short of a direct image. Second, measurement of gas emission can provide an independent estimate of the total mass of material currently in the disk, and thus an indication of the reservoir of material potentially available both to increase the mass of the central star via accretion, and to build a planetary system. Finally, at some stage, the solid material in the disk may agglomerate to form planetesimals. Observations of our own solar system suggest that at this stage, not all the gas will yet have been accreted by the star or incorporated into (giant) planets (e.g., Bodenheimer 1992). Hence, observations of gas as well as dust emission around solar-type stars spanning a range of ages can eventually place limits on how long significant masses of distributed small particles and gas survive in circumstellar disks, and can thus constrain estimates of the time scale available (*a*) for building planetesimals from small dust grains and (*b*) for accumulating gas into Jovian-like planets. Therefore, we have undertaken two parallel programs, the first aimed at detecting disk dust associated with young ($t < 3$ Myr) solar-type stars and their progeny in older ($t > 10$ Myr) clusters (Strom et al. 1989; Skrutskie et al. 1990), and the second at detecting disk gas (Skrutskie et al. 1991). In this contribution, we report an initial result from this second program: detection of a double-peaked CO profile characteristic of emission arising from a rotating circumstellar disk around the T Tauri star, GG Tau.

2. THE ENVIRONMENT AND PROPERTIES OF GG TAURI

We selected GG Tau for observation primarily because it lies in a region relatively devoid of ambient molecular line emission, near the outskirts of the nearby ($d = 140$ pc) Taurus-Auriga star-forming complex. This fortunate circumstance, which enables sensitive searches for circumstellar molecular gas with single-dish millimeter-wave antennae, is illustrated in Figures 1 and 2. Figure 1 shows a map of ^{12}CO antenna temperature against LSR velocity for a region of dimension 4.2 × 5′ surrounding GG Tau. These observations were obtained in 1991 June and 1992 April, with the 15 element QUARRY receiver (Erickson et al. 1992) at the Five College Radio Astronomy Observatory 14 m antenna. The beam FWHP at 115 GHz is $\theta = 45''$, and the spectra in Figure 1 are spaced at $\theta = 50''$ intervals. The observations were obtained in a position-switched mode with the off position located 10′ east of the source. The QUARRY pixel separation is 50″ in the EW direction and 100″ NS; two pointings of the telescope are thus required to produce a map sampled at one beamwidth inter-

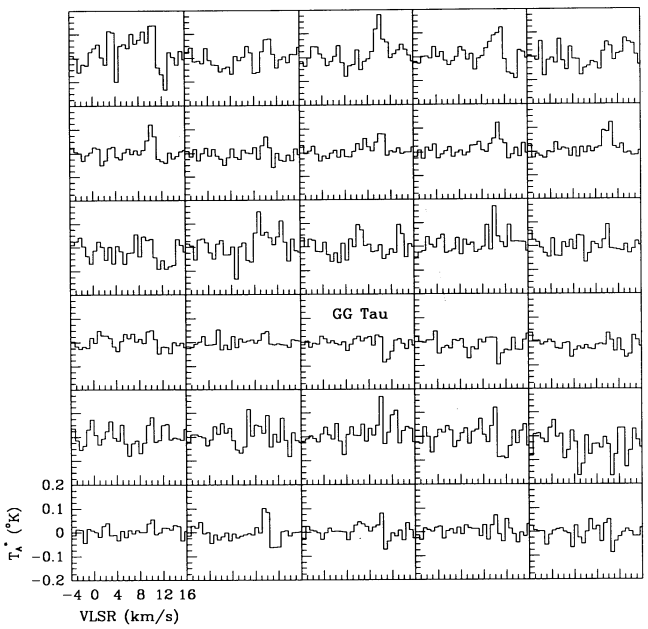

FIG. 1.—Map of ambient ^{12}CO $J = 1$–0 emission centered on GG Tau obtained with the 15 channel QUARRY receiver at FCRAO. The spacing between positions is 50″ in right ascension and declination. The upper limit to ambient emission at the velocity of GG Tau ($v_{LSR} = 6.2$ km s^{-1}) is 50 mK (3 σ).

vals. The on-source integration time was 3.7 hr for the set of 15 spectra with the central pixel located on GG Tau and was 1.1 hr for the second pointing, with the central pixel located 50″ north of GG Tau. The system temperature at ^{12}CO was typically 700 K. The systemic velocity of GG Tau determined from visible wavelength spectroscopy is $v_{LSR} = 5.3 \pm 2$ km s^{-1} (Herbig & Bell 1988). The Nobeyama ^{12}CO detection reported here yields $v_{LSR} = 6.2 \pm 0.1$ km s^{-1}. None of the individual QUARRY spectra shows evidence for ambient ^{12}CO emission at the GG Tau rest velocity; the upper limit at the map position centered on GG Tau is 50 K (3). However, a weak feature at $v_{LSR} = 10$ km s^{-1} appears in many of the spectra. This velocity is consistent with the velocity of ambient Taurus molecular cloud material in this direction (Ungerechts & Thaddeus 1987). Figure 2 illustrates the spatial average of the 30 spectra contributing to the map in Figure 1 and shows the

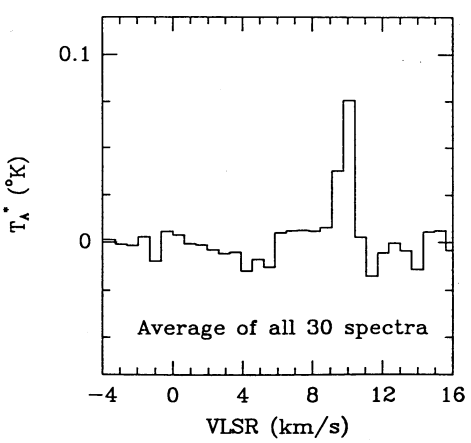

FIG. 2.—Average of the 30 ^{12}CO spectra presented in Fig. 1 showing ambient extended emission at $v_{LSR} = 10$ km s^{-1}. No extended emission is evident at the velocity of GG Tau (6.2 km s^{-1}) to a limit of 20 mK (3 σ).

$v_{LSR} = 10$ km s^{-1} feature more clearly. There is no evidence for ambient cloud emission *extended over the entire map* at the GG Tau rest velocity at a level which exceeds $T_A = 20$ mK (3 σ).

GG Tau is the brightest member of an optical pair of T Tauri stars (projected separation $\theta \sim 10''$, or $r \sim 1400$ AU at the distance of Taurus-Auriga).[5] The best available values (Hartigan et al. 1993) for spectral type and luminosity for GG Tau and its fainter companion are [M0, log $(L/L_\odot) = 0.28 \pm 0.1$] and [M5, log $(L/L_\odot) = -0.78 \pm 0.1$]. The masses and ages of the pair (based on comparison with the tracks published by VandenBerg et al. 1983) are $M \sim 0.7\ M_\odot$, $t \sim 1$ Myr, and $M \sim 0.3\ M_\odot$, $t \sim 3$ Myr for the brighter and fainter components of the pair respectively. Note that the NRO observations reported below refer to the brighter component of the pair. The infrared spectral energy distribution of the primary closely follows the $\lambda F_\lambda \sim \lambda^{-4/3}$ shape expected for a circumstellar disk (see Strom et al. 1989 and Beckwith et al. 1990 for a summary of recent observations); the magnitude of the observed infrared excess above photospheric levels suggests that the disk is heated both radiatively, by the central star, and viscously, via accretion. Its observed 1.3 mm continuum flux is among the largest measured among the sample of solar-type pre–main-sequence stars in Taurus-Auriga [F (1.3 mm) = 593 $\pm$ 53 mJy; Beckwith et al. 1990]. Based on observations with the Nobeyama Radio Observatory interferometer array, Ohashi et al. (1991) measure F (3 mm) = 41 $\pm$ 4 mJy within a region of dimension $\theta < 5''$. Simon & Guilloteau (1992) report resolution of the dust emission region surround GG Tau. Their observations with the IRAM interferometer at $\lambda = 2.6$ mm reveal (1) an elongated emission region centered on GG Tau of approximate dimensions $2'' \times 6''$, and (2) much weaker emission centered on its fainter companion. From the measured flux density of the extended emission centered on GG Tau, F (2.6 mm) = 80 mJy, combined with the 1.3 mm measurement reported by Beckwith et al. (1990), they deduce that the emitting region must be optically thin at 2.6 mm. For an assumed gas/dust ratio of 100, they estimate the mass of circumstellar gas to be $\sim 0.1\ M_\odot$. The relatively large gas mass implied by the millimeter-continuum measurements makes GG Tau an extremely attractive candidate for detecting disk gas emission.

3. NOBEYAMA RADIO OBSERVATORY OBSERVATIONS OF GG TAURI

Observations of the brighter components of the GG Tau system were obtained with the Nobeyama Radio Observatory (NRO) 45 m diameter telescope on 1992 March 2 in the ^{12}CO (1–0) and CS (2–1) transitions at 115.271204 and 97.980964 GHz, respectively. The nominal NRO beam size (FWHP) at these two frequencies is $\theta \sim 15''$ and $\theta \sim 17''$. The spectral resolution of the acousto-optical spectrometer (AOS) is 0.11 km s^{-1} at 115 GHz and the data are sampled at 0.052 km s^{-1} intervals. The baseline was established via position-switching to offset positions located 1′ E and 1′ W of GG Tau. The antenna temperature calibration was established by measuring a blackbody load inserted into the beam. Pointing was checked at least once per hour via offsetting to NML Tau while absolute calibration of the observations was established through measurements of the H II complex, W3. The sky conditions were clear, and the wind velocity did not exceed 5 m s^{-1} during the observing period. In Figure 3, we reproduce ^{12}CO profiles for two individual 40 minute integrations: (GG Tau—the off positon 1′ E and 1′ W respectively), along with the summed ^{12}CO line profile. The total on-source integration time was 80 minutes and the resulting rms noise is 70 mK per channel. *The summed ^{12}CO data, as well as each individual scan, exhibit a double-peaked profile.* The maximum antenna temperature in the summed profile is T_A (max) = 500 mK, while the velocity difference between the peaks is 1.1 $\pm$ 0.2 km s^{-1}; the full width at half-intensity is 2.4 $\pm$ 0.2 km s^{-1}. It is essential to note that the detected double-peaked profile appears to be associated with GG Tau itself (1) because T_A (max) and Δv are identical (to within the errors) for observations with two separate off positions, (2) the derived ^{12}CO velocity of 6.2 $\pm$ 0.1 km s^{-1} is identical to within the error of the photospheric velocity of GG Tau derived from optical measurements, (3) the line width, peak antenna temperature, and LSR velocity of the observed ^{12}CO profile differ significantly from those characterizing nearby regions within the Taurus-Auriga molecular complex, and (4) ambient extended emission (on a scale $> 10''$) centered on GG Tau would have been detected with ease at FCRAO in the course of our deep QUARRY observations.

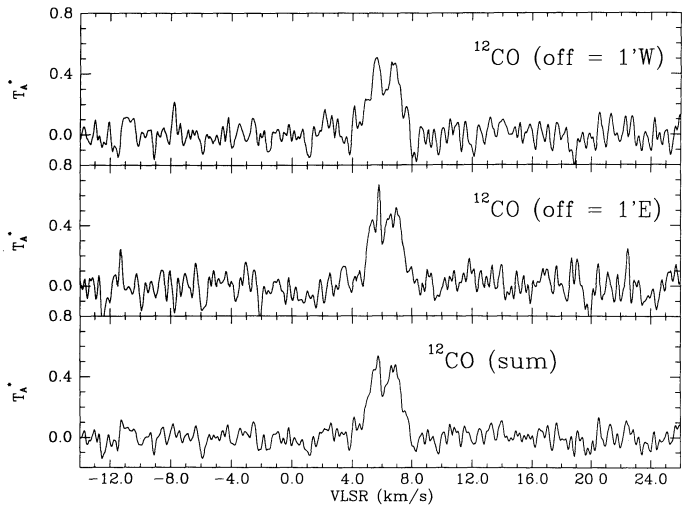

FIG. 3.—NRO ^{12}CO $J = 1$–0 profiles of GG Tau. The top two spectra are from independent 40 minute integrations on-source using different reference positions relative to GG Tau. The bottom profile is the average of the two spectra. Spectra have been boxcar-smoothed over an 0.21 km s^{-1} interval.

In Figure 4, we reproduce the summed ^{12}CO profile, and present as well the results of the CS (2–1) measurements obtained simultaneously. The summed CS measurements show no evidence of emission at the GG Tau rest velocity, and rms fluctuations of 31 mK per 0.1 km s^{-1} resolution element. In addition to these measurements, we attempted to detect C^{18}O (1–0) emission using the NRO 45 m telescope in 1992 April. The instrumental and atmospheric conditions during these observations were very similar to those reported above for the ^{12}CO and CS observations. The results of a 2 hr integration (shown in Fig. 4) show no evidence of emission from GG Tau, and RMS fluctuations of 24 mK per 0.1 km s^{-1} resolution element.

[5] Recently, Leinert et al. (1992) report the detection of close companions to each member of the optical pair based on speckle interferometry. The projected separations are $\theta \sim 0''.255$ and $\theta \sim 0''.93$, respectively, for the primary and secondary members of the pair. The observed monochromatic flux ratio of the brighter to fainter component is 1.6 at a wavelength $\lambda = 2.2$ μm.

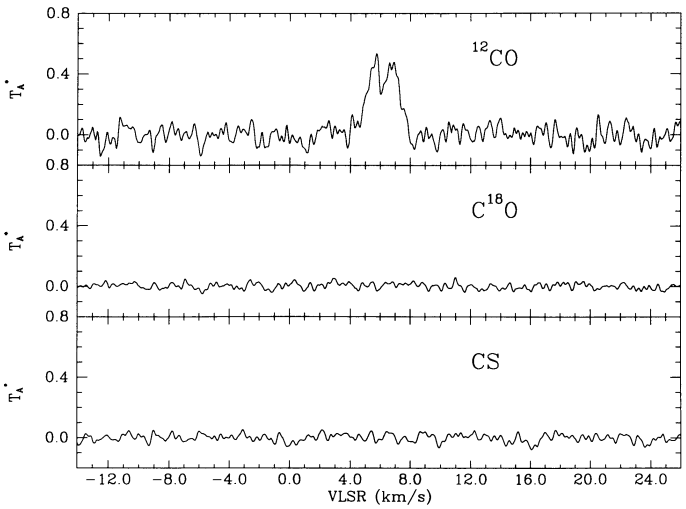

FIG. 4.—NRO ^{12}CO $J = 1$–0, C^{18}O $J = 1$–0, and CS $J = 2$–1 spectra of GG Tau. Spectra have been boxcar-smoothed over a 0.21 km s^{-1} interval.

4. MODELING THE OBSERVED LINE PROFILE

A double-peaked CO profile could arise (1) from an outflow or expanding shell of gas with terminal velocity ~ 2 km s^{-1}, (2) separate "blobs" of circumstellar CO with velocities differing by ~ 2 km s^{-1}, (3) self-absorption in a broad CO line, or (4) by emitting gas confined to a rotating circumstellar disk.

An expanding shell seems unlikely in view of the typical terminal velocities for outflows emanating from T Tauri stars. Both forbidden line widths and blueshifted P Cygni absorption profiles imply terminal velocities of ~ 200 km s^{-1} for T Tauri winds (e.g., Edwards et al. 1987). Observed molecular outflows (Snell 1989) have velocities of order 10 km s^{-1}, more akin to the velocity widths measured here; however such outflows are rarely observed toward optically visible T Tauri stars (Edwards & Snell 1984). Since the outflow emission arises from ambient gas swept up in an expanding flow from the star, most outflow sources, unlike GG Tau, exhibit a strong emission peak at the stellar rest velocity with weak wings arising from the outflow emission.

The superposition of a number of independent clouds could produce the observed double-peaked profile; however, invoking separate gas blobs within the beam to explain the observed profile seems artificial because (*a*) the average velocity of the gas is 6.2 ± 0.1 km^{-1} and thus is identical to within measurement errors of the stellar systemic velocity (5.3 ± 2 km s^{-1}) and (*b*) because the peaks are of identical height to within the observational errors.

Deeply embedded protostars sometimes exhibit self-absorbed line profiles (Lada & Wilking 1980); however, as was the case with molecular outflows, optically visible T Tauri stars rarely produce self-absorbed lines. Given the disk temperature profile inferred from infrared and millimeter continuum observations, the warm inner regions of the disk are too small to provide the warm background material for self-absorption. Cosmic-ray heating probably maintains the outer disk material at a uniform temperature.

Although one cannot definitively rule out any of the above possibilities, the observed CO profile can be modeled naturally in terms of emission arising from a rotating circumstellar disk; to first order, the line width will be twice the Keplerian rotation velocity in the outermost disk projected onto the line of sight. We have simulated a set of line profiles using a Monte Carlo program which assumes (1) that the disk gas is in Keplerian rotation about the central star, (2) that the disk has a uniform temperature, (3) that the disk optical depth decreases exponentially with increasing radius (although we experiment with other observations of the radial fall off of the optical depth), and (4) that the central object has a mass of 0.7 $M_\odot$. Note that if the subarcsecond companion reported by Leinert et al. (1992) indeed lies within the disk, then the total assumed stellar mass may have to be altered. To compute the CO profile, we divide the disk into a large number of parcels each specific by the radial distance from the star, r, and the azimuthal angle, θ. We then select (using a random number generator), a large number of (r, θ) pairs. For each pair, we compute the velocity of the disk gas (projected onto the line of sight), thus determining the "velocity bin" into which the flux from the disk will be added. The Monte Carlo simulation program then adds to this "bin" the product

$$re^{-0.7x^2/r_b^2}(1 - e^{-\tau(r)}) \quad (1)$$

where the first term, r, accounts for the area element $r\,d\theta$; the second term is the Gaussian antenna beam efficiency at radius, x, from the disk center as projected on the plane of the sky; r_b is the Gaussian half-power width of the telescope beam; and the final term includes the optical depth at radius r as determined by the assumption that the disk optical depth falls exponentially with a characteristic scale length r_s and has an optical depth of unity one scale length from the center. The simulation program then sums the contributions from n_t trials to produce a profile with a spectral bin separation of 0.05 km s^{-1} (identical to the sampling at NRO). Typical profiles are computed with $n_t = 500{,}000$ trials. We have compared the profiles computed using this idealized approach with the more detailed radiative transfer calculations of Beckwith & Sargent (1993) and find good agreement.

In Figure 5, we reproduce a set of disk models in which we vary i, the disk inclination angle (in our notation, $i = 90°$ is edge-on), and r_s simultaneously, while imposing the constraint that the computed profiles fit the observed line width. For any choice of i, the model fit to the observed profile determines the effective disk size, since most of the emitting solid angle is located at large radial distances. The results summarized in this figure can be understood by recalling that at high inclinations, where projection onto the line of sight decreases the apparent line width, the disk must have a *smaller* radius (higher Keplerian speeds) relative to the edge-on case in order to produce the same line width after projection onto the line of sight. In Table 1, we summarize for a selection of assumed system inclination angles the best fit values of a quantity r_0, the "half-power radius"; half the emission arises from radii $r < r_0$. Note that, for this particular model, r_0 also equals the radius of a sharply truncated optically thick disk which produces the same total emission. In addition to models in which we posit a

TABLE 1

DERIVED DISK RADIUS (r_0) VERSUS INCLINATION

Inclination	Radius (AU)	Angular Radius
80°	660	4.″7
60	600	4.2
45	440	3.2
30	200	1.4
15	60	0.4

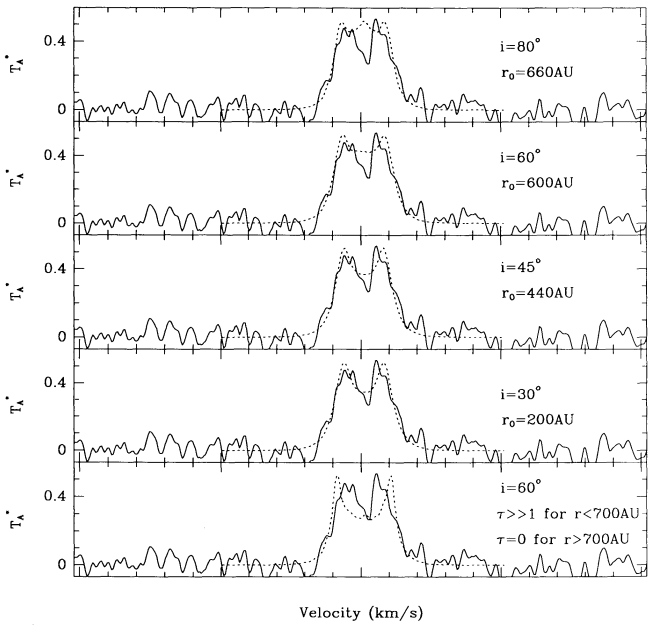

FIG. 5.—Series of model fits to the observed GG Tau ^{12}CO profile with rotating Keplerian disks of various inclinations and radii. The top four plots derive from a model in which the disk is optically thick out to a radius, r_s; afterward, the disk optical depth falls exponentially with a scale length, r_s. The last plot shows, for comparison, the effect of truncating an optically thick disk at an outer radius. In all cases the disk radius has been adjusted to match the observed linewidth.

smooth decrease of disk optical depth with radius, we have also run simulations in which we introduce an "edge" to an optically thick disk. An example is included in Figure 5 for a disk with $i = 60°$ and $\tau \gg 1$ out to a radius $r = 700$ AU. Note that a truncated disk produces sharp edges to the profile and peaks which lie close to the velocity extrema. Although the signal-to-noise ratio precludes a definitive statement, there is no hint of the expected behavior for a truncated disk. Hence, we conclude tentatively that the falloff of the disk optical depth with radius must be relatively smooth.

If the disk indeed extends smoothly to large distances from the star and is viewed at relatively high inclinations, the models predict that significant emission, arising from regions several disk exponential scale lengths from GG Tau, would fall outside the $\theta = 15''$ Nobeyama beam. The potential contributions from these regions is not negligible, because the increase in surface area compensates partially for the decrease in disk optical depth. Beam "truncation" leads to a reduction in the peaks in the double-peaked profile relative to the emission at the line center, owing to the exclusion from the beam of the most highly red- and blueshifted material from the outer edge of the disk. In extreme cases, when the disk is close to edge-on, the suppression of the line profile peaks yields a third peak at the profile center. The observed contrast between the profile peaks and emission near line center requires that $i < 60°$ in order that the best-fit disk radius be small enough to avoid signification "truncation" by the NRO beam, and thus favors moderate inclinations. In this regard, we note as well that the FCRAO upper limit on ^{12}CO emission suggests that little emission arises outside the NRO beam.

Even though inclinations near edge-on can be ruled out from the observed profile morphology, the range of disk radii derived from the profile shape alone still spans a significant range. However, the integrated flux provides an independent constraint on the disk size, assuming that the disk temperature and turbulent velocity are known quantities. To a good approximation, for a disk which is optically thick in ^{12}CO, the peak observed antenna temperature is

$$T_A = T_{\rm disk}\,\eta_{\rm beam}(v_{\rm turb}/2.4\ {\rm km\ s^{-1}})(\Omega_{\rm disk}\cos i/\Omega_{\rm beam})\,, \quad (2)$$

where $v_{\rm turb}$ is the turbulent velocity within the disk, $\eta_{\rm beam}$ is the beam efficiency, and $\Omega_{\rm disk}$ and $\Omega_{\rm beam}$ are the disk and beam solid angles, respectively (see Skrutskie et al. 1991). Rearranging the above equation yields

$$R = 850/(x\cos i)^{1/2}\ {\rm AU}\,, \quad (3)$$

where

$$x = T_{\rm disk}(v_{\rm turb}/2.4\ {\rm km\ s^{-1}})\,. \quad (4)$$

Here R is the radius of an optically thick disk which yields the required solid angle (analogous to r_0 in Table 1). The disk turbulent velocity is unknown. It must be less than 1 km s^{-1} to avoid disruption of the disk at the largest radii. Although the thermal line width of CO at 20 K is 0.2 km s^{-1}, the smallest CO line width observed in dark cloud cores is 0.3 km s^{-1} (Meyers, Ladd, & Fuller 1991). Thus, the gas in these cores has a significant nonthermal line width. We assume a disk turbulent velocity of order 0.5 km s^{-1} and plot in Figure 6 the variation of R as a function of inclination for disk gas temperatures of 10 and 20 K. The disk temperature is unlikely to be less than 10 K owing to cosmic-ray heating (Goldsmith & Langer 1978). The dashed lines in Figure 6 represent similarly derived upper limits from the FCRAO QUARRY nondetection. The fact that the solid lines all lie below the FCRAO limits is consistent with the nondetection at the facility. In this figure, we also plot the radii obtained from the line profile modeling from Table 1 (*solid points*). We conclude that our models are most consistent with the observed total emission for radii ranging from $400 < r_0 < 600$ AU for a disk temperature of 20 K. The corresponding inclinations range from $40° < i < 70°$. These disk radii and inclinations are close to

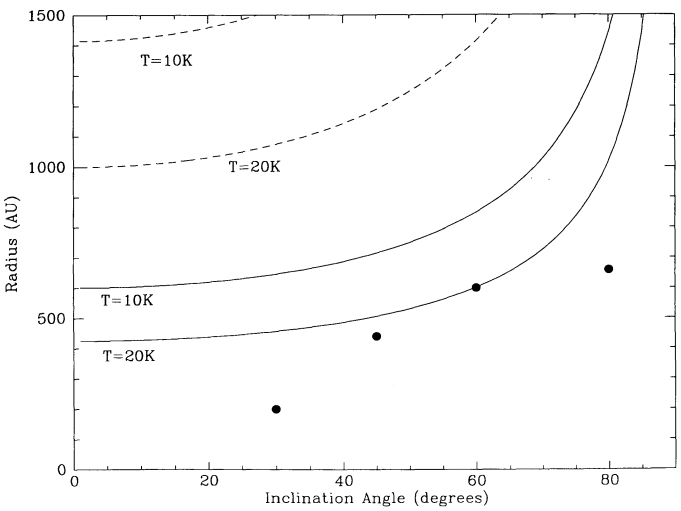

FIG. 6.—Observational constraints on disk radius vs. inclination which derive from ^{12}CO line flux (*solid lines*) and dynamical models of the line width (*points*). These independent constraints are most consistent for $400 < r_0 < 600$ AU and $40° < i < 70°$. The dashed lines represent the upper limits provided by the FCRAO QUARRY nondetection.

those derived from the 2.6 mm continuum imaging of Simon & Guilloteau (1992).

5. CONSTRAINTS ON THE GAS MASS AND CHEMICAL COMPOSITION

The ^{12}CO and $C^{18}O$ data can be used to place limits on the mass of gas (M_{gas}) surrounding GG Tau. A firm *lower limit* to M_{gas} can be established for the observed ^{12}CO emission if we assume that this line is optically thin. If the ^{12}CO excitation temperature T_{ex} is much greater than the cosmic background emission, and if the populations of the rotational levels are given by a Boltzmann distribution characterized by T_{ex}, then the total column density of CO averaged over the NRO beam is given by

$$N_{tot} = (4.15 \times 10^{13}) T_{ex} / e^{-5.54/T_{ex}} \int T_A/\eta_{beam}\, dv\ , \qquad (5)$$

where the integrated line intensity ($\int T_A/\eta_{beam}\, dv$) is in units of K km s^{-1}. Assuming a value of $N(H_2)/N(^{12}CO) = 10^4$, a beam angular diameter $\theta = 15''$, and a distance to GG Tau of 140 pc, the total gas mass is then given by

$$M_{gas}/M_\odot > 5.5 \times 10^{-7} T_{ex} / e^{-5.54/T_{ex}} \int T_A/\eta_{beam}\, dv\ . \qquad (6)$$

The observed integrated antenna temperature of the ^{12}CO emission from GG Tau is 1.0 K km s^{-1}. Correcting for the beam efficiency of the NRO telescope ($\eta_{beam} = 0.5$) yields a corrected integrated intensity of 2.0 K km s^{-1}. Thus, for an excitation temperature of 10 K, the gas mass, $M_{gas} > 2 \times 10^{-5}$ $M_\odot$. For higher excitation temperatures, the lower limit mass is greater. For example, with $T_{ex} = 30$ K, $M_{gas} > 4 \times 10^{-5}$ $M_\odot$.

Since the observed ^{12}CO emission may arise from an optically thick region, we can use the $C^{18}O$ detection limit to establish an *upper limit* on M_{gas} with the NRO beam. If we assume that the $C^{18}O$ emission is optically thin, in analogy to the ^{12}CO analysis, we can estimate the gas mass as:

$$M_{gas}/M_\odot < 3.4 \times 10^{-4} T_{ex} / e^{-5.28/T_{ex}} \int T_A/\eta_{beam}\, dv\ , \qquad (7)$$

where we have assumed a ratio $N(H_2)/N(C^{18}O) = 5 \times 10^6$. The 3 σ limit on the integrated intensity of the $C^{18}O$ line over the line width observed in ^{12}CO and corrected for the beam efficiency of the telescope, is 0.11 K km s^{-1}. For $T_{ex} = 10$ K and $T_{ex} = 30$ K, the upper limit on the mass of gas is 6.3×10^{-4} $M_\odot$ and 1.3×10^{-3} $M_\odot$, respectively. Assuming terrestrial isotope ratios, the maximum ^{12}CO optical depth consistent with the $C^{18}O$ nondetection is $\tau(^{12}CO) = 16$.

We note that our NRO measurements of the gas emission are probably dominated by regions which are large ($r \gg 100$ AU) in comparison to the solar system ($r \sim 50$ AU). The inner ($r < 50$ AU) regions of a disk might, in principle, contain arbitrarily large amounts of gas within an optically thick core. Owing primarily to beam dilution effects, such gas would not be detectable with the NRO in $C^{18}O$ emission nor add significantly to the observed ^{12}CO emission. This fact may account for the apparent discrepancy between the above results and the disk mass predicted from millimeter-continuum observations of the dust reported by Beckwith et al. (1990). On the other hand, the calculations of Beckwith et al. assume an interstellar gas-to-dust ratio. This ratio may not apply within a circumstellar disk. The measurements of Simon & Guilloteau (1992) spatially resolve the dust emission around GG Tau and find that emission is extended over a region of size comparable in extent to the value of r_0 deduced from our ^{12}CO observations. Their observations also suggest that the dust emission at millimeter wavelengths is optically thin. Since our measurements and those of Simon & Gilloteau derive from regions of similar spatial scale, we can estimate the mean gas-to-dust ratio. For constant temperature optically thin emission the mass of dust is given by

$$M_D = \lambda^2 d^2 S_\nu / (2kT\kappa_\nu)\ , \qquad (8)$$

where S_ν is the observed flux density and κ_ν is the mass absorption coefficient for the dust alone. Assuming $\kappa_\nu = 1$ cm^{-2} gm^{-1} (Beckwith et al. 1990; Simon & Guilloteau 1992), and dust temperatures of 10 and 30 K, the mass of dust is 2×10^{-3} $M_\odot$ and 6.7×10^{-4} $M_\odot$, respectively. The mass of dust is similar to the upper limits on the mass of gas implied by our CO observations, thus establishing an upper limit to the gas-to-dust ratio of order unity. If, however, the dust emission observed by Simon & Guilloteau arises from regions interior to the regions probed by our CO observations, then the true gas-to-dust ratio could be larger. This fact, combined with the uncertainty in κ_ν, suggests that these estimates may be uncertain by an order of magnitude. Nevertheless, even at the extreme, they suggest significant depletion of gas relative to interstellar abundances. This deficit of detectable gas may reflect either (1) that the gas is depleted or (2) that CO is no longer an accurate tracer of the gas mass, either because it is dissociated, frozen onto the grains, or because carbon is locked up in more complex molecules. Since the emitting region must be at least a few hundred AU in extent to produce a detection, these estimates apply only on this spatial scale. An optically thick region $\ll 200$ AU in extent could hide substantial quantities of gas and contribute little to the observed flux.

The nondetection of CS from GG Tau can be used to place an upper limit on the abundance of CS relative to CO. The 3 σ upper limit on the CS-corrected, integrated antenna temperature is 0.14 K km s^{-1}. Assuming that the ^{12}CO and CS emission are both optically thin and in LTE at 20 K leads to the following ratio of average CS to CO column density:

$$N(CS)/N(CO) = 0.0043 \int T_A(CS)dv \Big/ \int T_A(CO)dv\ . \qquad (9)$$

Using the observed ratio of integrated intensities leads to a 3 σ upper limit to the $N(CS)/N(CO)$ ratio of 1.8×10^{-4}. This limit is consistent with the measured abundance ratio (1.25×10^{-4}) in the dense core, TMC 2 in the Taurus cloud complex (Irvine, Goldsmith, & Hjalmarson 1987). However, the true ^{12}CO optical depth could be much larger. As discussed above, the $C^{18}O$ detection limit establishes an *upper limit* to the optical depth of the observed ^{12}CO emission of τ (^{12}CO) = 16. If the average optical depth of the CO emission is indeed closer to this maximum, then the abundance ratio would be $N(CS)/N(CO) < 1.3 \times 10^{-5}$, thus suggesting CS depletion by a factor greater than 10 as compared to dense molecular cloud gas. Similar depletions of CS are reported for the HL Tau disk by Blake, van Dishoeck, & Sargent (1992).

5. DISCUSSION AND CONCLUSIONS

We have made use of the Nobeyama Radio Observatory 45 m millimeter-wave antenna to detect double-peaked $^{12}CO(1–0)$ emission in the direction of the T Tauri star, GG

Tau. The observed CO profile can be modeled readily by assuming that the emission arises in a rotating circumstellar disk. Independent morphological and kinematic evidence for circumstellar gas surrounding GG Tau derives from contemporaneous observations by Koerner, Sargent, & Beckwith (1992). Simon & Guilloteau (1992) report the observation of extended millimeter continuum emission arising from warm dust. Our NRO observations are best fitted by assuming a disk of radius $400 < r < 600$ AU, inclined at $i < 60°$ (with the convention that $i = 0°$ corresponds to pole-on) to the line of sight. Thus, the gaseous component of the circumstellar disk surrounding this young ($t < 3$ Myr) solar-type star would extend well beyond the radius of the solar system, to dimensions comparable to the structure observed around Vega-like systems (e.g., β Pictoris). A *lower limit* to the gas mass of $M_{\rm gas} > 2 \times 10^{-5}\ M_\odot$ is derived from ^{12}CO emission, while our nondetection of C^{18}O places an upper limit $M_{\rm gas} < 1.3 \times 10^{-3}\ M_\odot$. A small ($R \ll 200$ AU) optically thick component could hide substantial quantities of gas and remain undetected. Simon & Guilloteau (1992) have made millimeter-continuum observations which constrain the quantity of dust located at regions $r \gg 100$ AU. Their results, combined with our upper limit to the gas mass yield a gas-to-dust ratio (by mass) which may be as much as a factor of 100 smaller than that characteristic of the interstellar medium. Either (1) the gas-to-dust ratio is abnormally low, or (2) CO may no longer be an accurate tracer of the gas mass, either because it is dissociated, frozen onto grains, or because carbon is locked up in more complex molecules. We note as well that arbitrarily large amounts of gas can remain undetected if the gas is confined to regions ($r \ll 200$ AU) small in comparison to the Nobeyama beam.

No emission at the frequency of the CS (2–1) transition was detected. Without a more stringent limit on the ^{12}CO optical depth than is available from our present observations, we cannot distinguish between a ratio N(CS)/N(CO) consistent with that characteristic of dense molecular cloud regions, and a depletion of CS by a factor > 10.

Recent speckle observations suggest that GG Tau may be a close (*projected* separation $\theta \sim 0\farcs255$) binary system. Our minimum derived disk radius of $r \sim 300$ AU is much larger than the nominal *projected* separation ($r \sim 38$ AU) of the two putative components of the GG Tau system, and thus present a possible dilemma: how could a disk survive tidal destruction beyond a radius comparable to the separation between two companions of roughly comparable mass (as judged by their relative 2.2 μm brightnesses)? If further observations confirm that GG Tau is indeed a close binary, then (*a*) the true separation of the stars must exceed the projected separation by a factor ≥ 10, or (*b*) any disk must be a circumbinary disk.

Because GG Tau appears to be a young star ($t < 3$ Myr) surrounded by a circumstellar accretion disk, and because it is located in a region of relatively weak ambient molecular cloud emission, it represents a potentially valuable laboratory (1) for identifying molecular species best suited to probing physical and chemical conditions during the earliest stages of disk evolution, and (2) for probing the detailed kinematic and density structure of circumstellar disks during their earliest evolutionary phases.

We wish to thank A. Sargent, S. Beckwith, M. Simon, and S. Guilloteau, and D. Koerner for communicating their OVRO and IRAM results to us prior to publication. C. Masson provided valuable comments on the manuscript. We (S. E. S., K. M. S., S. E.) acknowledge with gratitude support from the NASA Origins of Solar Systems Program, the NASA Planetary Astronomy Program, and the National Science Foundation. We (M. F. S., R. L. S.) also wish to acknowledge support by the NSF of the Five College Radio Astronomy Observatory.

REFERENCES

Adams, F. C., Emerson, J. P., & Fuller, G. A. 1990, ApJ, 357, 606
Adams, F. C., Lada, C. J., & Shu, F. H. 1987, ApJ, 312, 788
Appenzeller, I., Jankovics, I., & Ostreicher, R. 1984, A&A, 141, 108
Beckwith, S. V. W., & Sargent, A. I. 1991, ApJ, 381, 250
———. 1993, ApJ, 402, 280
Beckwith, S. V. W., Sargent, A. I., & Chini, R. S. 1990, AJ, 99, 924
Bertout, C., Basri, G., & Bouvier, J. 1988, ApJ, 330, 350
Blake, G. A., van Dishoeck, E. F., & Sargent, A. I. 1992, ApJ, 391, L99
Bodenheimer, P. 1992, in Protostars and Planets III, ed. E. H. Levy & M. S. Matthews (Tucson: Univ. of Arizona Press), in press
Edwards, S., Cabrit, S., Strom, S. E., Heyer, I., Strom, K. M., & Anderson, E. 1987, ApJ, 321, 473
Edwards, S., & Snell, R. 1984, ApJ, 261, 151
Erickson, N., Goldsmith, P. F., Novak, G., Grosslein, R. M., Viscuso, P. J., Erickson, R. G., & Predmore, C. R. 1992, IEEE Trans. Microwave Theory and Tech., 40, 1
Goldsmith, P. F., & Langer, W. D. 1978, ApJ, 222, 881
Hartigan, P., Strom, K. M., Strom, S. E., & Edwards, S. 1993, in preparation
Herbig, G. H., & Bell, K. R. 1988, Lick Obs. Bull., 1111
Hildebrand, R. H. 1983, QJRAS, 24, 267
Irvine, W., Goldsmith, P., & Hjalmoarson, S. 1987, in Interstellar Processes, ed. D. J. Hollenbach & H. A. Thronson (Dordrecht: Reidel), 561
Kenyon, S. J., & Hartmann, L. 1987, ApJ, 323, 714
Koerner, D. W., Sargent, A. I., & Beckwith, S. V. W. 1992, ApJ, submitted
Lada, C. J., & Wilking, B. A. 1980, ApJ, 238, 620
Leinert, Ch., Haas, M., Richichi, A., Zinnecker, H., & Mundt, R. 1991, A&A, 250, 407
Lynden-Bell, D., & Pringle, J. E. 1974, MNRAS, 168, 603
Meyers, P. C., Ladd, E. F., & Fuller, G. A. 1991, ApJ, 372, L95
Ohashi, N., Kawabe, R., Hayashi, M., & Ishiguro, M. 1991, AJ, 102, 2054
Sargent, A., & Beckwith, S. 1991, ApJ, 382, L31
Simon, M., & Guilloteau, S. 1992, ApJ, 397, L47
Skrutskie, M. F., Dutkevitch, D., Edwards, S., Strom, S., & Strom, K. 1990, AJ, 99, 1187
Skrutskie, M. F., Snell, R., Dutkevich, D., Strom, S. E., Schloerb, F. P., & Dickman, R. L. 1991, AJ, 102, 1749
Snell, R. 1989, in Structure and Dynamics of the Interstellar Medium, ed. G. Tenorio-Tagle, M. Moles, & J. Melnick (Berlin: Springer-Verlag), 231
Strom, K., Strom, S., Edwards, S., Cabrit, S., & Skrutskie, M. F. 1989, AJ, 97, 1451
Ungerechts, H., & Thaddeus, P. 1987, ApJ, 63, 645
Weintraub, D. A., Sandell, G., & Duncan, W. D. 1989, ApJ, 340, L69
VandenBerg, D. A., Hartwick, F. A., Dawson, P., & Alexander, D. R. 1983, ApJ, 266, 747